



THE APPLICATION OF MICROPERFORATED MATERIAL TO CONTROL AXIAL FAN NOISE

Seungkyu LEE and J. Stuart BOLTON

*Ray W. Herrick Laboratories, School of Mechanical Engineering,
Purdue University, 177 South Russell Street,
West Lafayette IN 47906-2099, USA*

SUMMARY

In this paper, a passive fan noise control approach implemented by applying microperforated materials to the shroud of an axial fan will be discussed. Microperforated panels with different flow resistances were compared to an unperforated fan housing. In addition to the shroud treatment, the application of an extended microperforated housing to the inlet-end and outlet-end of the fan will be discussed.

INTRODUCTION

The axial fan is one of the most widely used devices for cooling electronic devices such as computers, home appliances, etc. An axial fan creates significant amounts of noise, which is generated by various flow interactions depending on where the fan is located during its operation. Unavoidable tonal and broadband noise can be created during the operation of an axial fan as a result of flow interaction between the housing and the blades, inlet and outlet flow interference due to the operating environment, flow separation, vortex shedding, etc.

Many studies have been conducted aimed at reducing fan noise by using various approaches. Gresho [1], Wang and Huang [2], and Lee et al. [3], focused on the structural design of the fan, such as the struts supporting the fan hub which could generate noise by interacting with the flow exiting from the rotor. Gregor et al. [4] conducted research on the impact of the axial fan guard grille design. Quinlan [5], Gee and Sommerfeldt [6], and Schulz et al. [7] studied active noise control techniques to reduce axial fan noise. Lee et al. [8] showed that axial fan noise could be reduced by introducing apertures in the housing to which the fan was mounted, which had the effect of reducing the fan's radiation efficiency.

In this paper, experimental research aimed at the attenuation of the noise generated in the tip clearance region of a fan will first be described. A number of researchers have already conducted

research on controlling the noise generated in the tip clearance region. Jin et al. [9] focused on the design of the fan blades, while Gorny et al. [10] conducted research on blade passage tone cancellation by installing a perforated resonator within the housing of the fan. The present work follows most closely that of Sutliff and Jones who investigated the beneficial effect of a foam-metal liner placed in close proximity to turbine blade-tips [11]. The purpose of the present research was to find the potential effect of a finite flow resistance, microperforated housing in reducing noise at the blade passage frequency generated in the tip clearance region. The sound power radiated by modified fans was measured to determine the effectiveness of various microperforated materials.

In addition to the MPP housing treatment around the blade-tip region, the effect of an extended inlet-end and outlet-end of the MPP-treated housing of the axial fan was also considered. This extension of the housing, in effect, placed the fan in the middle of a circular duct. The blade passage tone attenuation performance of the MPP duct casing was then studied.

EXPERIMENTAL SET-UP

The experimental set up required to test the noise generated by a 120 mm axial fan was created by following the procedures and equipment described in ISO 3744 [12], ISO 3745 [13] and ISO 10302-1 [14]. ISO 10302-1 is the construction manual for building the mylar plenum that was designed to allow estimation of both radiated fan noise and fan performance. The same ISO document also describes procedures to measure the sound power that is radiated from the noise source. ISO 3744 and ISO 3745 provide methodologies for setting up a microphone array around the noise source in a semi-anechoic chamber and for measuring the sound power level.

The mylar plenum for the fan noise experiment was built following the description provided in ISO 10302-1. The plenum was designed to allow accurate measurements of the flow rate and static pressure generated by the specimen fan. The flow rate and static pressure inside the plenum generated by the fan can be adjusted by changing the outlet opening area of the plenum. Figure 1 shows the drawing of the plenum as provided in ISO 10302-1.

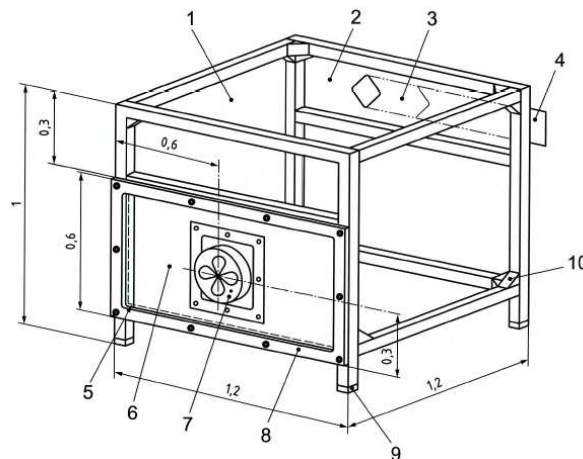


Figure 1 ISO 10302-1 mylar plenum design for accurate measurement of fan noise level and performance.

In order to measure the sound power radiated from the fan attached to the mylar plenum, a hemispherical microphone array was built. The dimension of the hemispherical frame and the locations of the microphones on the frame were determined by following ISO 3744. The configuration of the frame and the microphones locations are shown in Figure 2.

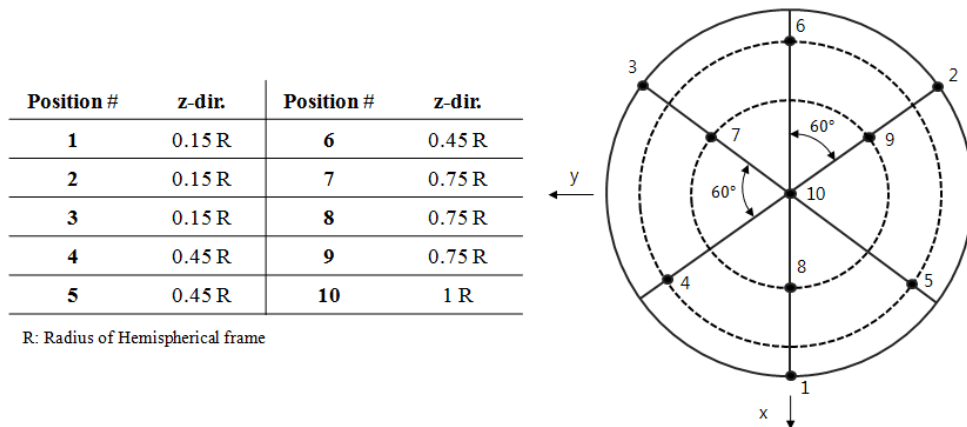


Figure 2 10 microphone positions used to measure the sound power radiated from the fan.

The sound power radiated by the fan under different operating conditions was measured using a combination of both the plenum and the hemispherical microphone array. The measurement was conducted in an anechoic chamber with a hard floor installed, thus making the space semi-anechoic. Figure 3 shows the actual experimental set up for the fan noise measurement.



Figure 3 Test setup in the anechoic chamber at the Ray W. Herrick Laboratories, Purdue University.

MICROPERFORATED PANEL APPLICATION

Three different microperforated panels (MPP's) were used as fan shroud materials in the present work, and the sound power level in each case was measured using the experimental set-up described in the previous section. Figure 4 shows the materials that were used to create the fan housings. The non-perforated material, which is denoted as "Impermeable" in the figure will be referred to as the "regular" casing in this paper. The other three materials, denoted as MPP 751, MPP 1204 and MPP 1759 in the figure, refer to the MPP's that were used in the experiments. The numbers after MPP indicate the nominal flow resistance of each material in $N \cdot s/m^3$.

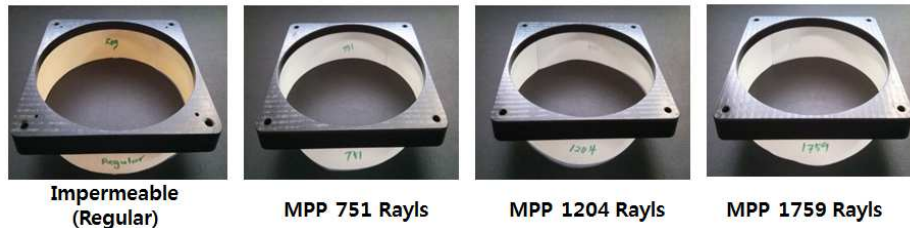


Figure 4 Materials used for the shroud materials of the fan. (Rayls = $N \cdot s/m^3$)

The specimen 120 mm axial fan was modified to insert the shroud materials. The modification of the fan and the assembly of the fan with MPP included is shown in Figure 5.

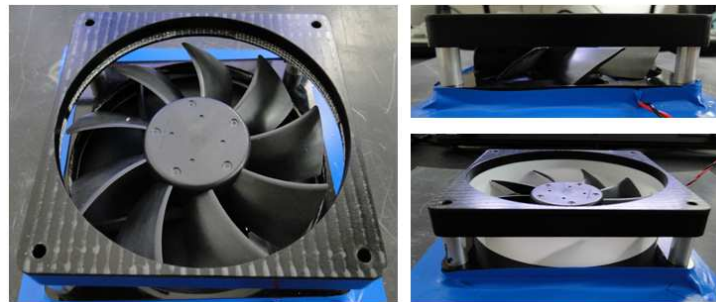


Figure 5 Modified fan to allow insertion of the microperforated material.

PERFORMANCE CURVE OF THE FAN

For a fair comparison of the sound power radiated from the fans with different housing materials, each fan with different housing material needs to be run under the same operating conditions. Therefore the operating conditions were selected over the entire performance curve of the fan. Figure 6 shows the different operating conditions, from 1 to 15, on the pressure-flow rate curves of the fans with the regular casing and microperforated casings; measurements were made using the plenum described in previous section at each of these operating points. The flow resistance of the microperforated panel used to obtain the performance curve shown below was $751 N \cdot s/m^3$.

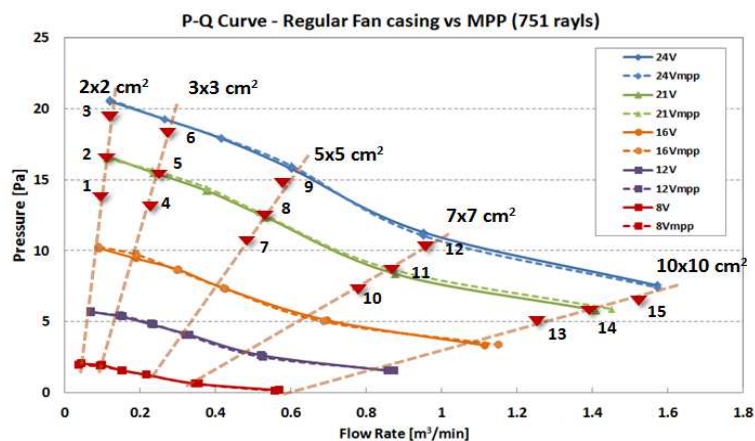


Figure 6 Performance curve of the fan. Pressure-Flow rate curve.

It can be seen from the performance curves in the Figure 6 that the performance of the fan made using the microperforated housing was essentially the same as the performance of the fan with the regular shroud.

SOUND POWER LEVEL MEASUREMENT

The sound power level radiated from the fan can be estimated from the sound pressure level that was measured by each microphone on the hemispherical frame shown in Figure 3. In the measurement of the sound pressure level at each microphone position, Brüel and Kjaer type 4189 and type 4190 microphones were used. Sound pressure signals were recorded while running the fan at each operating condition; 120 seconds of data were recorded at a sampling rate of 25.6 kHz. The recorded signal obtained from each microphone was divided into segments with a 50% overlap and a Hann window was applied to each segment, and then the power spectral density calculation was applied to each of the overlapped and windowed signals. Sound pressure spectral levels were thus calculated at the ten microphone positions.

After the sound pressure level measurements, the sound power level of the fan was calculated using the following equation:

$$L_w = \bar{L}_p + 10 \log_{10} \frac{S}{S_{ref}} \quad (1)$$

where, \bar{L}_p is the space-averaged sound pressure level at the ten microphone positions, S is the surface area of the hemisphere and S_{ref} is the reference area, 1 m².

RESULTS FOR DIFFERENT BLADE-TIP HOUSING MATERIALS

The fans with different casings were tested under the fifteen different operating conditions as indicated in Figure 6, and in Table 1. In this paper, comparisons at a few of the operating conditions will be illustrated graphically, and the blade passage tone levels at all of the operating conditions will be provided in tabular form. The selected operating conditions for the comparison studies for this paper are tabulated in Table 2. The measured sound power level spectra in the blade passage frequency region for different fan housing materials were compared along with the cumulative spectrum for each housing material. The cumulative spectrum can be obtained by integrating the area under the sound power level spectrum and it is an effective tool for visualizing the strength of tonal components embedded in a sound power level spectrum.

Table 1 Blade Passage Frequency for each operating condition. (BPF – Blade Passage Frequency).

Operating Points	Opening Area [cm ²]	BPF [Hz]	Operating Points	Opening Area [cm ²]	BPF [Hz]	Operating Points	Opening Area [cm ²]	BPF [Hz]
1	2 x 2	221.2	6		260.5	11		262.2
2		239.9	7	5 x 5	231.5	12		282.3
3		257.5	8		242.8	13	10 x 10	237.1
4	3 x 3	223.9	9		260.5	14		256.8
5		242.8	10	7 x 7	240.9	15		277.5

Table 2 Operating conditions of the fan selected for comparison studies between different materials.

	Condition 1 (Pt. #2)	Condition 2 (Pt. #6)	Condition 3 (Pt. #7)	Condition 4 (Pt. #14)
Pressure (Pa)	16.5	18.2	10.5	5.91
Flow rate (m³/min)	0.11	0.27	0.48	1.39

Figure 7 shows the sound power level and the cumulative sound power spectra of fans with different housing materials in the blade passage frequency region. Recall that each frequency point of the cumulative sound power level represents the overall sound power level created by frequency components at and below that frequency. The cumulative spectrum thus provides a clear visualization of the blade passage tone level differences that result from using different shroud materials in the fan.

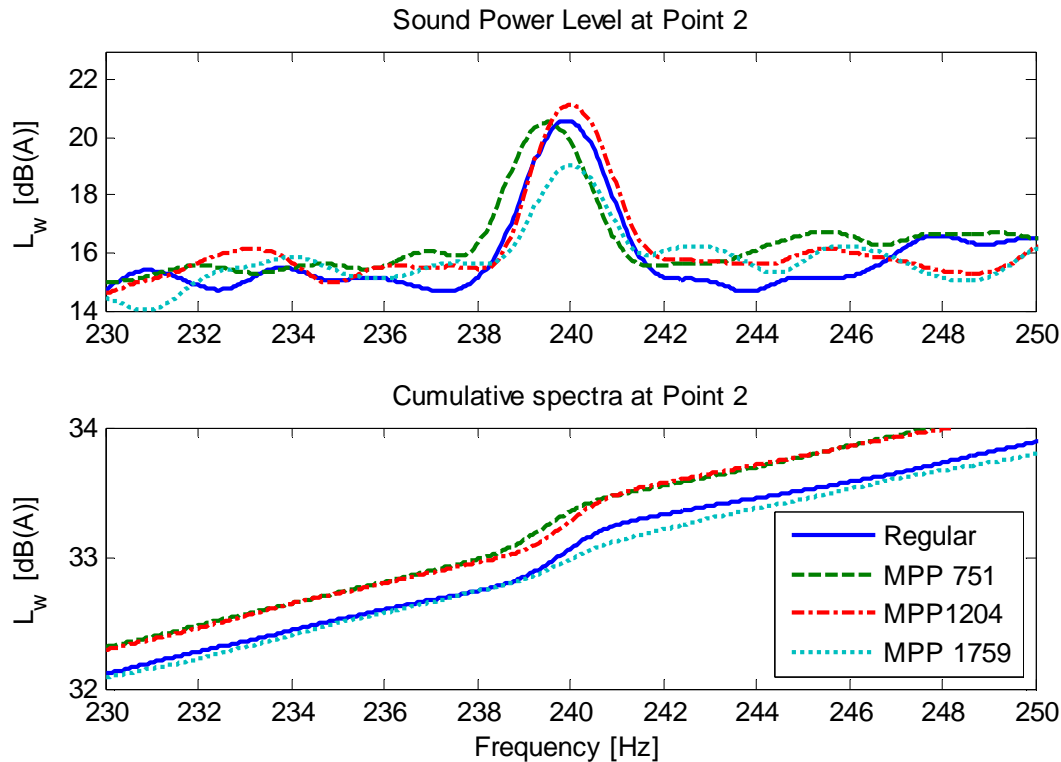


Figure 7 Sound power level and cumulative spectra at $P=16$ Pa, $Q=0.11\text{m}^3/\text{min}$.

In the first case, the operating condition of the fan was point 2 in the P - Q curve in Figure 6. When the fan operates under this condition, it generates a low flow rate and high static pressure. It can be seen that the microperforated panel that has the flow resistance $1759\text{ N}\cdot\text{s}/\text{m}^3$, which is the highest flow resistance of the materials tested, shows the best performance in reducing the blade passage tone. Note that the “step” in the cumulative spectrum at the blade passage frequency in the bottom figure of Figure 7, also shows that the $1759\text{ N}\cdot\text{s}/\text{m}^3$ flow resistance MPP results in the lowest overall sound pressure level. In contrast, MPP’s with lower flow resistances such as $751\text{ N}\cdot\text{s}/\text{m}^3$ and $1204\text{ N}\cdot\text{s}/\text{m}^3$ increased the blade passage tone of the fan in comparison with the regular housing. Therefore it can be concluded that a relatively high flow resistance is required for the microperforated housing of the 120 mm axial fan in this performance range.

Figure 8 shows the results when the fans with different housing materials were run at the operating condition 6 in Figure 6. This condition represents a low flow rate ($0.27\text{ m}^3/\text{min}$) and very high pressure region (18.2 Pa) in the performance curve. This operating condition can be achieved by adjusting the opening area of the plenum in Figure 1 to 4 cm^2 . It can be seen from the figure that the MPP with $1204\text{ N}\cdot\text{s}/\text{m}^3$ flow resistance reduced the blade passage frequency tone the most, and by looking at the cumulative spectra, the overall sound power level at the blade passage frequency tone was also the lowest among all the fans. Therefore in this particular operating condition, the MPP having a flow resistance of $1204\text{ N}\cdot\text{s}/\text{m}^3$ was the most suitable for the housing material.

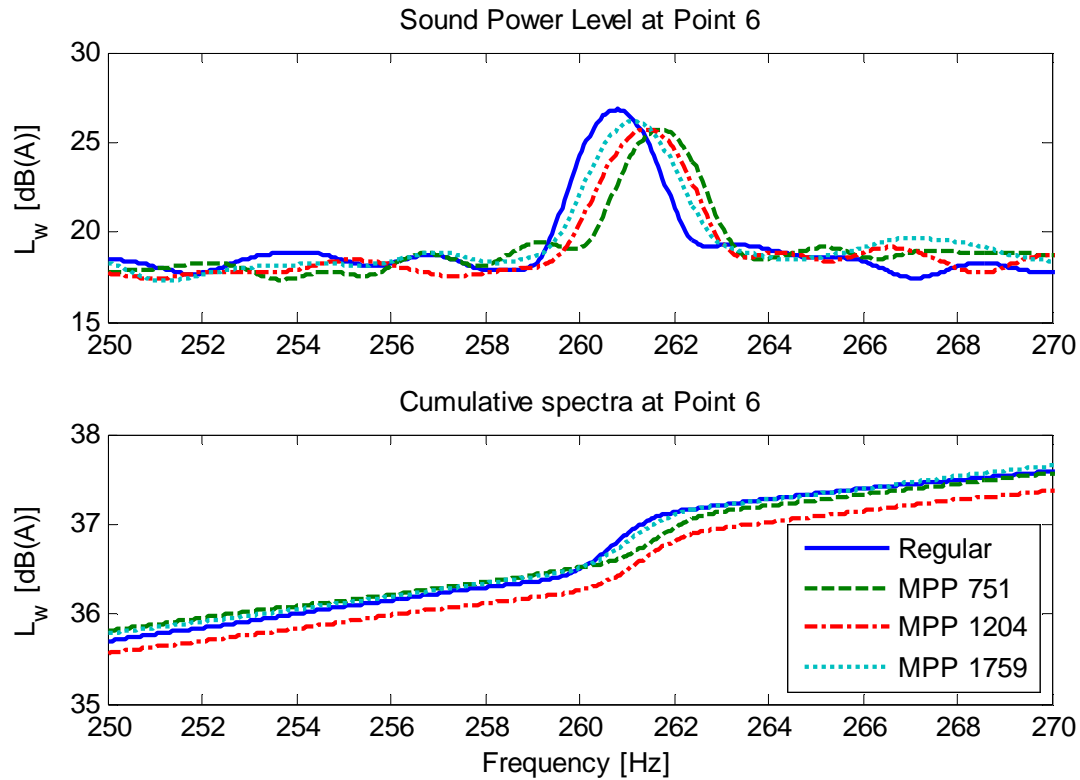


Figure 8 Sound power level and cumulative spectra at $P=18.2$ Pa, $Q=0.27$ m³/min.

Figure 9 shows the results for the fan running under operating condition 7, which is a low flow rate (0.48 m³/min) and medium pressure region (10.5 Pa). This condition can be achieved by adjusting the opening area of the plenum to 25 cm². In contrast with the results in Figures 7 and 8, the MPP with a flow resistance of 751 N·s/m³ resulted in the lowest blade passage tone. Moreover, the overall sound power level was also the lowest with that microperforated panel.

Finally, Figure 10 shows the acoustical measurements of the fans with different housing materials at operating condition 14. This condition represents a low pressure (5.91 Pa) and very high flow rate (1.39 m³/min) region. From the sound power level spectra, it can also be seen that MPP 751 N·s/m³ gives the best performance in blade passage tone level reduction. Moreover, the cumulative spectra also indicate that the MPP 751 N·s/m³ reduces the blade passage tone the most even though the MPP 751 N·s/m³ has higher broadband noise levels than other housing materials.

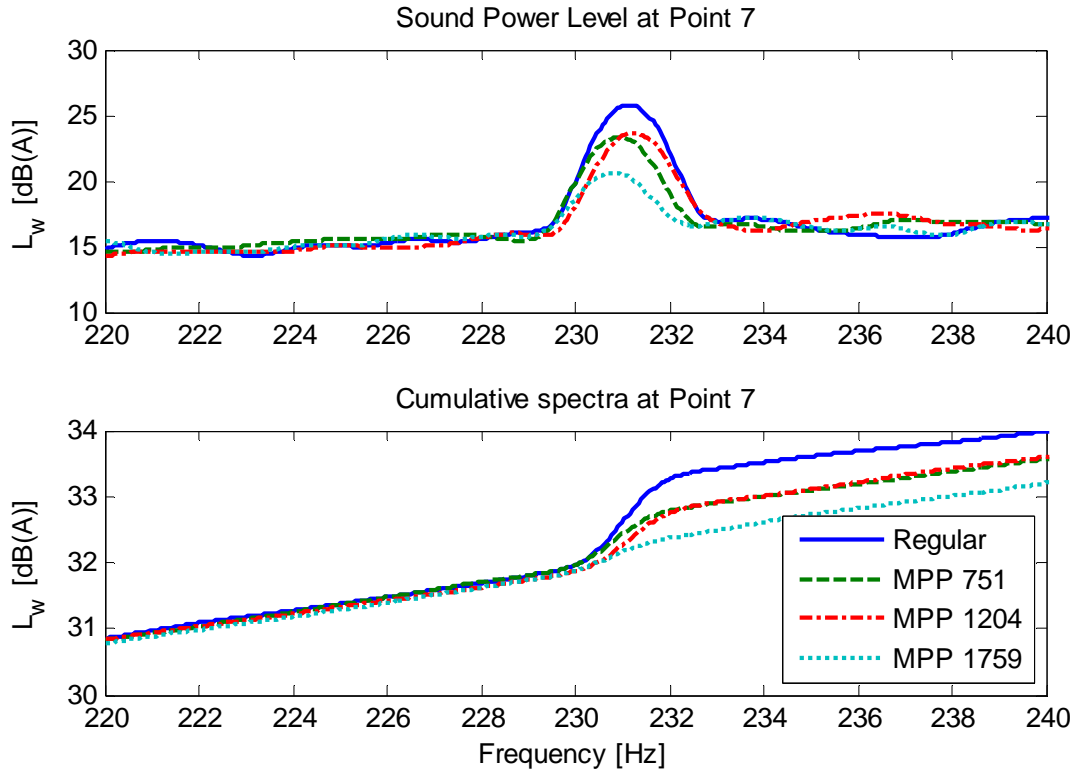


Figure 9 Sound power level and cumulative spectra at $P=10.5$ Pa, $Q=0.48$ m³/min.

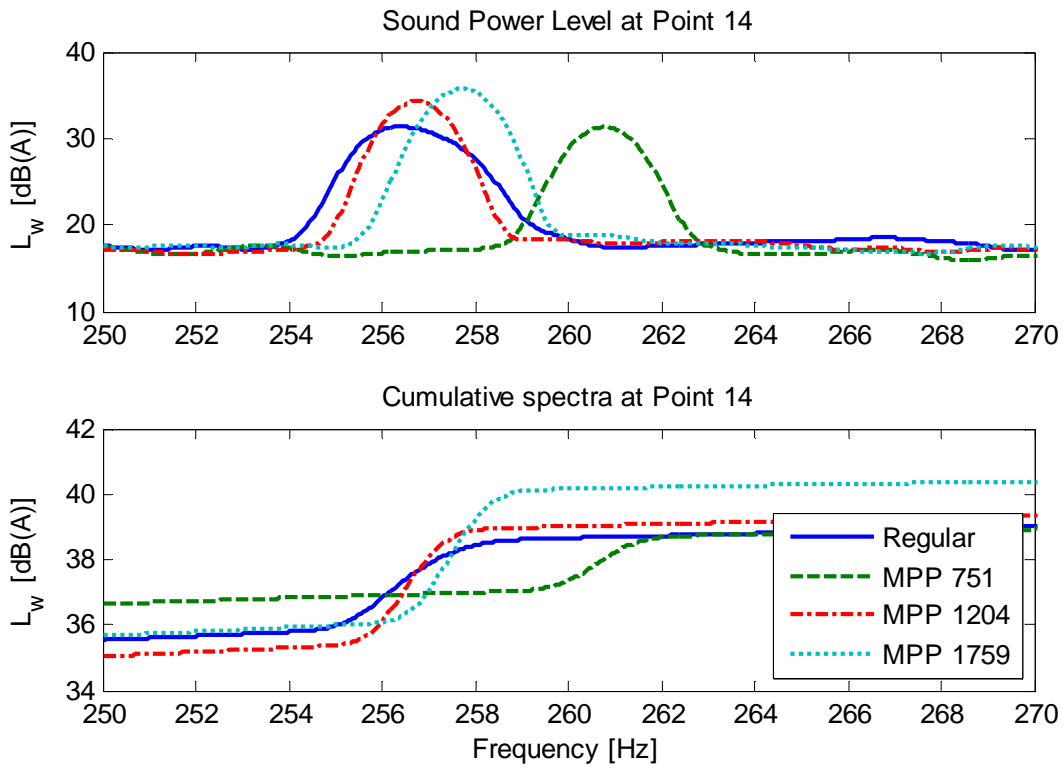


Figure 10 Sound power level and cumulative spectra at $P=5.91$ Pa, $Q=1.39$ m³/min.

The blade passage frequency tone levels for all materials and operating conditions are tabulated in Table 3. The MPP casing with 1759 N·s/m³ flow resistance shows the best performance in reducing the blade passage frequency tone at operating conditions 1 through 3. This region represents the very low flow rate region, which can be found along the 2×2 cm² opening area line in the *P-Q* curve. The results at conditions 4 through 6, which are located on the 3×3 cm² line in the performance curve show that the MPP casing with 1204 N·s/m³ flow resistance reduced the blade passage tone level the most in this region of the performance map. The MPP casing with 751 N·s/m³ of flow resistance shows the best performance in reducing the blade passage tone over the rest of the performance curve. The latter operating condition points correspond to generally larger opening areas such as 5×5 cm², 7×7 cm² and 10×10 cm².

Table 3 Blade Passage Tone levels for all cases. Lowest tones were highlighted in red.

(OP# - Operating Condition Points)

OP #	Blade Passage Tone Level [dBA]				OP #	Blade Passage Tone Level [dBA]				OP #	Blade Passage Tone Level [dBA]			
	Reg	751	1204	1759		Reg	751	1204	1759		Reg	751	1204	1759
1	17.45	17.14	17.86	15.89	6	27.06	26.18	23.42	24.57	11	27.30	24.82	26.47	27.84
2	20.59	20.54	21.15	19.03	7	27.59	23.03	27.51	26.09	12	29.16	27.09	27.24	29.38
3	22.76	23.54	23.89	21.09	8	29.58	26.19	30.46	27.85	13	30.34	24.86	30.48	34.75
4	21.02	19.11	17.33	18.95	9	31.26	28.09	32.35	29.70	14	31.37	29.63	34.26	35.71
5	24.01	23.32	21.24	21.50	10	24.54	22.11	23.33	25.19	15	34.50	31.28	34.81	37.32

FAN WITH MICROPERFORATED DUCT

In this section, the radiation of sound power from an axial fan that is surrounded with an extended inlet and outlet microperforated panel (MPP) duct will be considered. Figure 11 shows the configuration of the fan with the microperforated duct. The extension of the MPP housing element to the inlet and outlet of the axial fan is expected to suppress the dipole-like sound source of the axial fan.

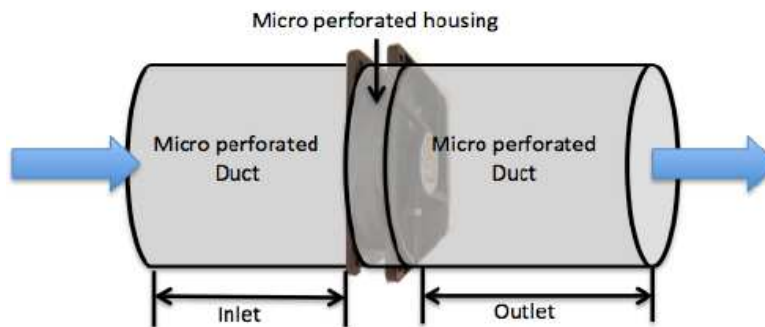


Figure 11 Configuration of the fan with inlet and outlet extended microperforated duct.

The experimental study of the sound power measurement of a ducted fan was also made following the procedure described in ISO 10302-1. The sound power radiated from the fan with the extended microperforated duct was compared with the fan with a normal sized microperforated housing. The microperforated material used for this comparison study was MPP 751, which showed good blade passage tone attenuation for most operating conditions. The extended lengths of the duct of the inlet

and outlet were each 6 cm so the total length was 12 cm. The operating conditions for the comparison studies illustrated graphically below were conditions 2 and 4 from Table 2.

Figure 12 shows the sound power level spectra and cumulative spectra comparisons between the regular MPP housing and the MPP duct housing at operating point 6 from Figure 6. “MPP 751 Blade Tip housing” denotes the fan with microperforated panel housing only around the blade tip-region of the fan and “Duct MPP 751 housing” denotes the extended microperforated panel housing case. It can be seen that the extended inlet and outlet MPP duct housing not only reduces the blade passage tone at this operating condition but also reduces the broadband noise, particularly at low frequencies. Figure 13 also shows that the MPP housing, when extended, creates better attenuation at the blade passage tone level as well as of the broadband noise at operation point 14.

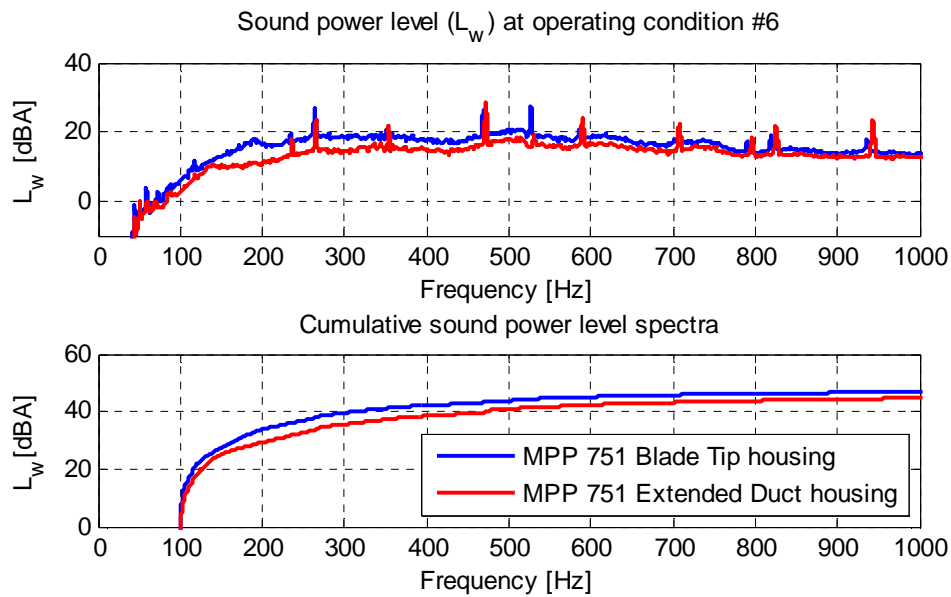


Figure 12 Sound power level comparison between MPP 751 regular casing and duct casing at operating condition #6.

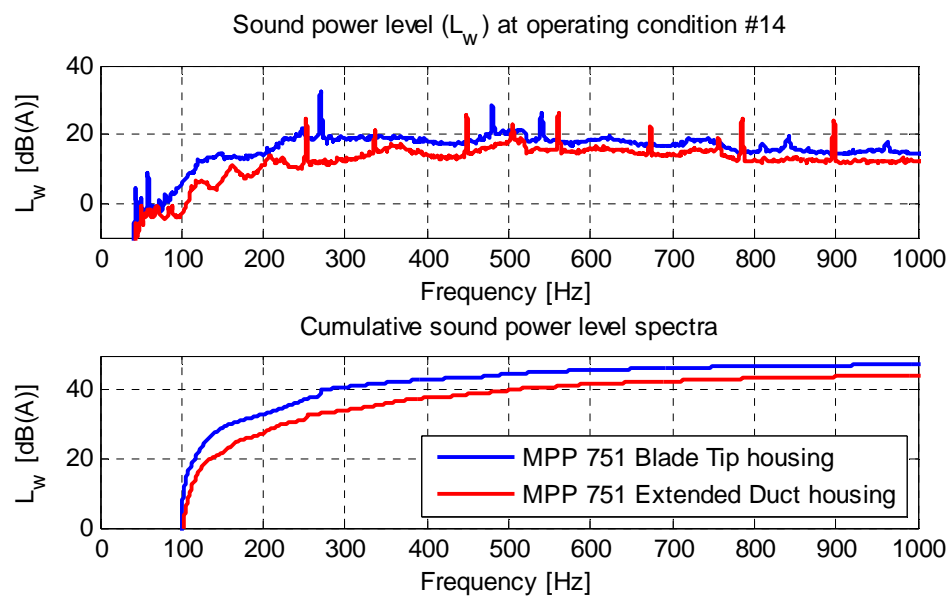


Figure 13 Sound power level comparison between MPP 751 regular casing and duct casing at operating condition #14.

The blade passage tone level comparison results for all of the operating conditions are tabulated in Table 4. As shown in the table, the MPP duct shows better attenuation performance at the blade passage tone of the axial fan in all cases, in some cases by as much as 9 dB. It was also found that the MPP duct was advantageous from a flow point-of-view. Figure 14 shows the $P-Q$ curve of the MPP duct and the regular MPP 751 housing fan. In the higher flow rate regions, especially, the fan with the MPP duct produces more static pressure than the regular MPP cased fan. This means that when both fans operate at the same rotation speed, the fan with the microperforated duct produces more static pressure.

Table 4 Blade Passage Tone levels for all cases.

OP #	Blade Passage Tone Level [dB(A)]		OP #	Blade Passage Tone Level [dB(A)]		OP #	Blade Passage Tone Level [dB(A)]	
	REG 751	DUCT 751		REG 751	DUCT 751		REG 751	DUCT 751
1	20.09	18.32	6	26.75	23.51	11	24.51	21.04
2	23.67	21.94	7	24.86	16.71	12	26.67	24.43
3	26.98	23.78	8	27.90	18.81	13	29.57	21.73
4	20.93	17.95	9	30.40	22.29	14	32.19	24.29
5	24.46	20.59	10	24.37	18.53	15	27.66	27.66

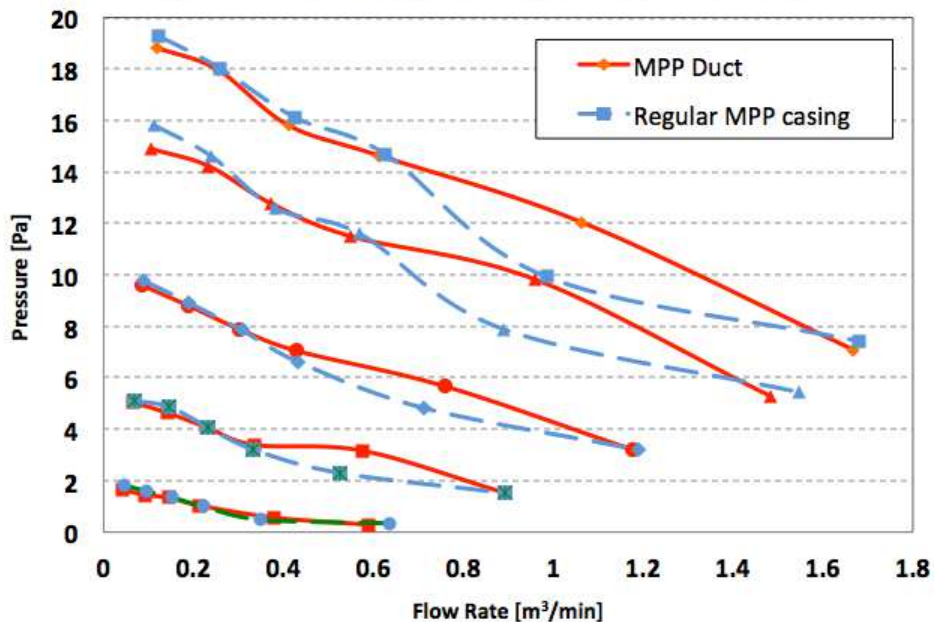


Figure 14 $P-Q$ curve comparison between the regular MPP751 casing and the MPP duct (DUCT751).

CONCLUSION

In this research, detailed experiments to reveal the effects of microperforated materials in reducing 120 mm fan noise were conducted. A repeatable and fair measurement procedure was established which gave reliable results showing that different microperforated treatments are preferred in different fan operating conditions. It can also be seen from the ducted fan noise measurement that the MPP treatment as a duct is effective for blade passage tone attenuation compared to the MPP housing treatment just around the normal blade-tip region of the fan. Moreover, an extended housing as a duct is beneficial from a flow point-of-view.

In further studies, different lengths and flow resistance of the microperforated duct will be considered. In addition to that, more detailed studies to visualize the sound around the axial fans with different housing materials and sizes will be made by adopting Nearfield Acoustic Holography (NAH).

ACKNOWLEDGEMENT

The authors acknowledge the support of 3M Corporation through the provision of materials for the axial fan noise measurements and for the financial support of this work.

BIBLIOGRAPHY

- [1] W.M. Gresho – *The reduction of impeller-strut interaction noise on small tube-axial fans*. INCE Conference Proceedings NOISE-CON 85, Columbus, OH, USA, **1985**
- [2] J. Wang, and L. Huang – *Quantification and control of noise sources in a small axial-flow fan*. Noise Control Engineering Journal 54(1), 27-32, **2005**
- [3] S. Lee, G-S Lee, S. Heo and C. Cheong - *Computation of internal aeroacoustics of axial freezing fan in refrigerators*, Proceeding of INTER-NOISE 2008, Shanghai, China, **2008**
- [4] A. Gregor, M. Hocevar and B. Sirok - *Study of axial fan grilles noise and aerodynamic characteristics*, Proceeding of INTER-NOISE 2009, Ottawa, Canada, **2009**
- [5] D.A. Quinlan - *Application of Active Control to Axial Flow Fans*, Noise Control Engineering Journal 39(3), 95-101, **1992**
- [6] K.L. Gee and S.D. Sommerfeldt - *A compact active control implementation for axial cooling fan noise*, Noise Control Engineering Journal 51(6), 325-334, **2003**
- [7] J.W. Schulz, W. Neise and M. Moser - *Active control of the blade passage frequency noise level of an axial fan with aeroacoustic sound sources*, Noise Control Engineering Journal 54(1), 33-40, **2006**
- [8] M. Lee, J.S. Bolton, T. Yoo, H. Ido and K. Seki –*Fan noise control by enclosure modification*, Proceeding of INTER-NOISE 2005, Rio de Janeiro, Brazil, **2005**
- [9] G. Jin, H. Ouyang, Y. Wu and Z. Du - *Effect of skewed blades on tip-clearance for different flow rates in axial fan*, Noise Control Engineering Journal 59(4), 320-332, **2011**
- [10] L. Gorny, G.L. Koopmann, W. Neise and O. Lemke - *Modeling of adaptively tunable flow driven resonators for axial fan blade tone noise attenuation*, Proceeding of INTER-NOISE 2007, Reno, Nevada, **2007**

- [11] D.L. Sutliff and M.G. Jones - *Low-Speed Fan Noise Attenuation from a foam-metal liner*, Journal of Aircraft 46(4), 1381-1394, **2009**
- [12] ISO 3744, *Acoustics – Determination of sound power levels of noise sources using sound pressure – Engineering method in an essentially free field over a reflecting plane*, **1994**
- [13] ISO 3745, *Acoustics –Determination of sound power levels and sound energy levels of noise sources using sound pressure - Precision methods for anechoic rooms and hemi-anechoic rooms*, **2012**
- [14] ISO 10302-1, *Acoustics –Measurement of airborne noise emitted and structure-borne vibration induced by small air-moving devices*, **2011**